



Published in final edited form as:

*J Cardiovasc Pharmacol.* 2020 March ; 75(3): 259–267. doi:10.1097/FJC.0000000000000789.

## Restoration of Adiponectin-Connexin43 Signaling Mitigates Myocardial Inflammation and Dysfunction in Diabetic Female Rats

Korin E. Leffler, PhD, Abdel A. Abdel-Rahman, PhD, FAHA

Department of Pharmacology and Toxicology, East Carolina University, Brody School of Medicine, Greenville, NC

### Abstract

Our preclinical findings replicated women's hypersensitivity to type-2 diabetes mellitus (T2DM)-evoked cardiac dysfunction along with demonstrating estrogen (E<sub>2</sub>)-dependent disruption of the cardiac adiponectin (APN)-connexin43 (Cx43) signaling. Whether the latter molecular anomaly underlies this women's cardiovascular health problem remains unknown. We hypothesized that restoration of the disrupted APN-Cx43 signaling alleviates this sex/E<sub>2</sub>-dependent cardiac dysfunction in diabetic female rats. To test this hypothesis, we administered the adiponectin receptor 1 (AdipoR1) agonist AdipoRon (30 mg/kg/d for 10 days) to female sham operated (SO) and ovariectomized (OVX) rats, which exhibited and lacked the T2DM left ventricular (LV) dysfunction, respectively, when fed high fat diet and received low dose streptozotocin regimen; non-diabetic control SO and OVX rats received control diet and vehicle for streptozotocin. In T2DM SO rats LV dysfunction, AdipoRon mitigated: (i) LV hypertrophy, (ii) reductions in fractional shortening (FS), LV developed pressure, dP/dt<sub>max</sub>, dP/dt<sub>min</sub>, and Tau. In LV tissues of the same rats, AdipoRon reversed reduction in Cx43 and elevations in TNF $\alpha$ , heme-oxygenase 1 (HO-1) and circulating cardiovascular risk factor Asymmetric Dimethylarginine (ADMA). The findings also revealed ovarian hormones independent effects of AdipoRon, which included dampening of the pro-oxidant enzyme HO-1. These novel findings yield new insight into a causal role for compromised APN-Cx43 signaling in the E<sub>2</sub>-dependent hypersensitivity to T2DM-evoked cardiac inflammation and dysfunction. Equally important, the findings identify restoration of Cx43 signaling as a viable therapeutic modality for alleviating this women's cardiovascular health related problem.

---

Corresponding Author: Abdel A. Abdel-Rahman, PhD, FAHA, Department of Pharmacology and Toxicology, East Carolina University, Brody School of Medicine, Greenville, NC 27834, Phone: 252-744-3470, abdelrahmana@ecu.edu.

Authorship Contributions

Participated in research design: Leffler and Abdel-Rahman.

Conducted experiments: Leffler

Performed data analysis: Leffler

Wrote or contributed to the writing of the manuscript: Leffler and Abdel-Rahman

The authors declare no conflict of interest.

## Introduction

Studies are needed to understand the mechanisms of the hypersensitivity of women (1) and female rats (2) to type-2 diabetes mellitus (T2DM) associated cardiac anomalies despite their inherent estrogen ( $E_2$ )-mediated cardioprotection (3). Counterintuitively, our findings linked  $E_2$ -dependent disruption of adiponectin (APN)-connexin43 (Cx43) signaling to cardiac dysfunction in a model of T2DM (2). However, it remains unknown if such disruption plays a causal role in this women's cardiovascular health related problem.

$E_2$  regulation of the estrogen receptor (ER) subtypes contributes to sex differences in cardiovascular health and anomalies via modulation of redox enzymes and anti-inflammatory modulators (4). Specifically, while ER $\alpha$  upregulation contributes to the higher antioxidant catalase and ALDH<sub>2</sub> activities in healthy  $E_2$ -replete rats (5), ER $\alpha$  is paradoxically upregulated in dysfunctional cardiac myocytes of  $E_2$ -replete diabetic female rats (2). Further,  $E_2$  increases expression of cardiac g-protein coupled estrogen receptor (GPER) in female diabetic rats (2). It is likely these molecular responses contribute to dysregulation of APN in females (6).

Despite its  $E_2$ -dependent higher levels in healthy rats (7, 8), T2DM female rats exhibit greater falls in APN than their male counterparts (2, 9). While the APN receptors (AdipoR1, AdipoR2 and T-cadherin) mediate cardioprotection and display gender differences in certain tissues, their roles are poorly understood, particularly in diabetic females. It is noteworthy that reduced APN signaling may constitute an important missing link in our understanding of the mechanisms of the adverse cardiac outcomes of T2DM (10).

APN induction of the major cardiomyocyte connexin, Cx43 (11), constitutes a promising therapeutic target for alleviating heart diseases (12, 13) because Cx43 reduction plays more significant role in cardiac pathologies than previously thought (14). Specifically, Cx43 reduction in T2DM female rats along with cardiac dysfunction (2) provide clinically relevant framework for investigating the potential therapeutic benefits of restoring APN-Cx43 signaling in diabetic females.

While AdipoRon, an orally active small molecule agonist for AdipoR1 and Adipo2, represents a possible therapeutic for T2DM (15), its potential cardioprotective effect and its mechanism of action have not been studied in  $E_2$ -replete diabetic females. AdipoRon mediation of the effects of endogenous full molecular weight APN, such as activation of AMPK signaling, in both male and female mice (15) likely mediates AdipoRon attenuation of post-ischemic myocardial apoptosis (16), pressure overload-evoked cardiac remodeling (17, 18), and diabetic nephropathy (19). It is notable that Cx43 enhances the phosphorylation and cardioprotective function of Akt (20), and that ovarian hormones influence the roles of Cx43 (2) and pAkt (21) under different experimental conditions.

The goal of the present study was to test the hypothesis that restoration of APN-Cx43 signaling by AdipoRon mitigates sex/ $E_2$ -dependent exacerbation of cardiac dysfunction and the index of LV stiffness, Tau, in diabetic females. A second goal was to discern the ovarian hormones/ $E_2$  dependent and independent molecular responses triggered by this signaling

pathway to identify novel therapeutic targets for this women's cardiovascular health related problem.

## Materials and Methods

### Animals

Eight week old Wistar rats (Female; 170-200g, Charles River Laboratories, Raleigh, NC) were pair housed in standard plastic cages in the animal care center for the university. Free access to water and chow (Prolab Rodent Chow; Granville Milling, Creedmoor, NC) was allowed until the beginning of the special phytoestrogen-free diet. Rats received ad libitum control (AIN-93G Growth Purified diet; 57W5 TestDiet) or high fat (DIO Rodent Purified diet with 45% energy from fat; 58V8 TestDiet) diet (Granville Milling, Creedmoor, NC) as reported (2). University animal facility lighting was kept on a 12/12 hour light-dark cycle and with temperature maintained at  $23 \pm 1^\circ\text{C}$ , and humidity at  $50 \pm 10\%$ . Isoflurane anesthesia was used for conducting OVX and echocardiography. Ketamine and xylazine (90/10 mg/kg, respectively) anesthesia was utilized for the terminal femoral catheterization surgery. All surgical procedures along with pre- and post-operative analgesia (meloxicam 1mg/kg, 0.2ml/day, P.O.) were approved by the Institutional Animal Care and Use Committee (IACUC) and conducted in accordance with the Guide for the Care and Use of Laboratory Animals as adopted by the U.S. National Institute of Health and the National Research Council Committee Update of the Guide for the Care and Use of Laboratory Animals, 2015.

### Ovariectomy

Ovariectomy (OVX) was conducted as reported in our previous studies (2, 22). In summary, female rats were anesthetized with an isoflurane/oxygen gas mix (see above) and electric clipper flank shaved. The surgical area was prepped three times in a prone position with a povidone-iodine scrub and 70% ethanol cleanse. A 1.5 cm (approximate) skin layer incision was made and 1 cm incisions on either side of the underlying muscle from the second to fifth lumbar vertebrae. Ovaries were located via the muscle incision, tied off with three surgical knots and removed. The muscle was closed using absorbable sterile suture (Roboz Surgical Instrumental Co., Gaithersburg, MD), skin closed with surgical clips (Mikron Precision Inc., Gardena, CA) and removed 10-14 days later.

### Induction of type 2 diabetes mellitus (T2DM)

We adopted the high fat diet plus two low doses streptozotocin (STZ) regimen (23, 24), used in our recent study (2), to induce T2DM (Figure 1). Four weeks after the initiation of the special diet regimen, rats were injected with freshly prepared STZ (35 mg/kg; I.P.) in 0.1M citrate buffer (pH 4.0) or the buffer alone (control). A second STZ injection was given one week after the first injection under the same conditions. Three days post second STZ injection, non-fasting blood glucose levels were measured and recorded by a Blood Glucose Monitoring System (Freestyle-Precision Neo, Abbott, Alameda, CA) with tail vein blood and diabetes mellitus onset was identified by BGL  $\geq 250$  mg/dL. All experimental groups (including OVX) underwent the same T2DM induction protocol (Figure 1).

## Echocardiography

Baseline and biweekly echocardiography measurements were conducted, recorded and analyzed. Rats were anesthetized with isoflurane/oxygen (see above). A chemical depilator removed chest wall hair and skin was cleansed with warm water. Acoustic gel (non-toxic) was placed on the chest wall and ultrasound image recordings of the heart were collected and stored for analysis (Visual Sonics Vevo 3100 Imaging System, FujiFilm and VevoLab Software v.2.1.0, Toronto, Ontario, Canada). M-mode and B-mode images of LV end-diastolic diameter, interventricular septum and posterior LV wall thicknesses at end diastole were measured and averaged over five beat cycles. Further, we measured the relaxation constant Tau, which reflects LV chamber stiffness (25) in all groups.

## Intravascular catheterization

As described in previous studies (2, 26), a catheter consisting of 5 cm PE-10 tubing bonded to 15 cm PE-50 tubing was inserted into the abdominal aorta via left femoral artery under ketamine/xylazine anesthesia. After arterial catheters were connected to Gould-Statham (Oxnard, CA) pressure transducers and flushed with heparinized saline (100 IU/ml) via ML870 (AD Instruments, PowerLab 8/30; Colorado Springs, CO), blood pressure (BP) recordings were collected and analyzed by LabChart (v.8) pro software (AD Instruments, Colorado Springs, CO).

## Blood and tissue collection

At the conclusion of hemodynamic measurements, prior to sacrifice, blood was collected in heparinized tubes and centrifuged for 10 minutes at 2000g. Serum was collected and stored at  $-80^{\circ}\text{C}$  for biochemical analysis. Hearts were excised, weighed and flash frozen in 2-methylbutane (Sigma-Aldrich, St. Louis, MO) on dry ice. Tissue was stored at  $-80^{\circ}\text{C}$  until processed for ex vivo biochemical studies.

## Western blot analysis

All Western blots were conducted following the established protocols in our lab (2, 26). LV tissue was homogenized on ice in lysis buffer (20mM Tris, pH 7.5, 150mM NaCl, 1mM EDTA, 1mM EGTA, 1% Triton X-100, 2.5mM sodium pyrophosphate, 1mM beta-glycerophosphate, 1mM activated sodium orthovanadate and 1 $\mu\text{g}/\text{ml}$  leupeptin with a protease inhibitor cocktail (Roche, Indianapolis, IN), sonicated and centrifuged (12,000g for 20 min). Extracted supernatant protein was quantified using Bio-Rad protein assay system (Bio-Rad Laboratories, Hercules, CA). Protein extracts (40  $\mu\text{g}/\text{lane}$ ) were separated in a 4-12% gel electrophoresis (Novex Tris-Glycine gel; Life Technologies, Carlsbad, CA) at 175 V (Bio-Rad Laboratories, Hercules, CA). After semidry transfer to nitrocellulose membrane for 30 minutes at 25 V, 1 A (Bio-Rad Laboratories, Hercules, CA), membranes were blocked for 2 hours at room temperature in Odyssey blocking buffer (LI-COR Biosciences, Lincoln, NE). Post first blocking, membranes were incubated in primary antibody overnight at  $4^{\circ}\text{C}$  on a rocker. The primary antibodies used were as follows: Rabbit polyclonal anti-APN (#ab62551), TNF $\alpha$  (#ab6671), HO-1 (#ab13243), AdipoR1 (#ab126611), GPER or GPR30 (#ab137479) and anti-ER $\alpha$  (#ab3575) (all 1:200 dilution, Abcam, Cambridge MA). Rabbit polyclonal anti-AKT (#9272) (1:200 dilution, Cell

Signaling Technology, Danvers MA), Goat polyclonal anti-Cx43 (#ab87645) (1:200 dilution, Abcam, Cambridge MA) and Mouse monoclonal anti-GAPDH (#ab125247) (1:1000 dilution, Abcam, Cambridge, MA) and Mouse anti-pAKT (#4051) (1:200 Cell Signaling Technology, Danvers MA).

After primary antibody incubation, membranes underwent three PBS+ 0.1% tween washes and incubated with secondary antibody. Secondary antibodies were prepared (1:5000) with IRDye680-conjugated goat anti-mouse and IRDye800-conjugated goat anti-rabbit, or IRDye680 conjugated donkey anti-mouse and IRDye800-conjugated donkey anti-goat for sixty minutes on a rocker under dark conditions at room temperature. “Arbitrary units” refer to the target protein normalized to respective GAPDH on the same gel, or the phosphorylated (pAKT) protein to its respective total protein. Odyssey Infrared Imager was utilized for band detection and quantified by integrated intensities with Odyssey application software version 3 (LI-COR Biosciences, Lincoln, NE).

### Measurements of Asymmetric Dimethylarginine

For indication of cardiovascular risk, Asymmetric Dimethylarginine (ADMA) serum levels were measured, in duplicate, at the termination of the study with a commercially available ADMA ELISA rat-specific kit (MyBioSource, San Diego, CA) according to manufacturer’s instructions.

### Protocols and experimental groups

Six groups of rats (n=7 each), comprising 3 sham operated (SO) and 3 ovariectomized (OVX) groups, were divided into 3 pairs as follows: (i) non-diabetic SO and OVX, (ii) diabetic AdipoRon-treated SO and OVX and (iii) diabetic vehicle-treated SO and OVX groups. The tissues from non-diabetic groups were obtained from rats used in our earlier study (2). Baseline echo was obtained prior to the initiation of the studies and performed biweekly in all groups. After the second STZ dose, four weeks were allowed for the development of the type 2 diabetic state and AdipoRon (30 mg/kg/d; P.O.) or vehicle was administered during the last 10 days of this 4-week period (Figure 1). AdipoRon has an IC<sub>50</sub> of 1.8µM for AdipoR1 and 3.1µM for AdipoR2 (15). Thereafter, terminal arterial catheterizations were performed for hemodynamic measurements and studies concluded with euthanasia and tissue collection (Figure 1).

### Data analysis and statistics

Statistical analysis consisted of two-way ANOVA with post hoc F-test and Tukey’s unpaired t-test for significant findings. Values are expressed as means ± SEM with probability levels below 0.05 considered significant. Prism 7 software (Graphpad Software Inc., San Diego, CA) was used to perform statistical analysis.

## Results

### AdipoRon ameliorated LV hypertrophy in T2DM SO female rats

Non-diabetic OVX rats were heavier (P<0.05) than non-diabetic SO rats, and AdipoRon (30 mg/kg/d; 10 days) had no effect on body weight (Figure 2A). LV mass was higher (P<0.05)

in T2DM SO, but not in T2DM OVX rats, when compared to their respective non-diabetic controls, and AdipoRon mitigated ( $P<0.05$ ) this hypertrophy (Figure 2B). Ejection fraction was not affected by T2DM in SO or OVX rats but was decreased ( $P<0.05$ ) by AdipoRon in T2DM SO rats (Figure 2C).

### **AdipoRon mitigates cardiac dysfunction in T2DM SO female rats**

AdipoRon restored fractional shortening (FS) in T2DM SO rats while the lower FS in non-diabetic OVX rats was not affected by T2DM in the absence or presence of AdipoRon (Figure 2D). Similarly, reductions in LV developed pressure ( $P<0.05$ ) (LVDP; Figure 3A), and  $dP/dt_{\min}$  ( $P=0.001$ ) (Figure 3D) along with the increase ( $P<0.05$ ) in the LV relaxation constant Tau (Figure 3B), observed in T2DM SO, but not in T2DM OVX, rats were all reversed by AdipoRon. Trending reductions in  $dP/dt_{\max}$  (Figure 3C) in T2DM SO and reductions in T2DM OVX ( $P<0.05$ ) were reversed by AdipoRon in both groups.

### **AdipoRon reverses ER $\alpha$ upregulation, heightens GPER upregulation and restores cardiac Cx43 levels in T2DM SO females**

T2DM upregulated ( $P<0.05$ ) cardiac ER $\alpha$  in SO and OVX rats, compared to non diabetic controls, and AdipoRon reversed this upregulation (Figure 4A). AdipoRon further upregulated ( $P<0.05$ ) GPER (Figure 4B) and restored ( $P<0.05$ ) Cx43 to control levels (Figure 4C) only in T2DM SO females. T2DM reduced ( $P<0.05$ ) pAKT in SO, but not in OVX, rats (Figure 4D); AdipoRon had no further effect in T2DM SO rats, but reduced ( $P<0.05$ ) pAKT in T2DM OVX rats (Figure 4D).

### **AdipoRon suppresses cardiac expression of AdipoR1 and APN**

In T2DM SO, the reduction in cardiac AdipoR1 was exacerbated ( $P<0.05$ ) by AdipoRon and in T2DM OVX rats, the unaltered cardiac AdipoR1 was reduced ( $P<0.05$ ) by AdipoRon treatment (Figure 5A, C). Consistent with previous studies (2), T2DM reduced ( $P<0.001$ ) cardiac APN in SO and OVX rats and AdipoRon caused further cardiac APN reduction ( $P<0.05$ ) (Figure 5B and C).

### **AdipoRon treatment diminished elevations in ADMA and TNF $\alpha$ in T2DM SO females**

Non-diabetic OVX rats exhibited a trended increase in serum asymmetric dimethylarginine (ADMA; Figure 5D) and higher ( $P<0.05$ ) cardiac TNF $\alpha$  level (Figure 6A, C), compared with nondiabetic SO rats. T2DM increased ADMA in both SO and OVX ( $P<0.05$ ), but only increased TNF $\alpha$  in SO ( $P<0.05$ ). AdipoRon mitigated these elevations in T2DM SO vs. little or no effects in T2DM OVX rats (Figures 5D, 6A, C). In contrast, increases ( $P<0.05$ ) in cardiac heme-oxygenase 1 (HO-1) levels were similar in T2DM SO and T2DM OVX rats and were reversed in both groups by AdipoRon (Figure 6B).

## **Discussion**

The present study provided new knowledge on ovarian hormones dependent and independent mechanisms for T2DM-evoked cardiac dysfunction and its alleviation by restoring the cardiac APN-CX43 signaling. First, ovarian hormone-dependent reduction in cardiac Cx43 level is a major cause for heightened proinflammatory milieu and cardiac



dysfunction in T2DM SO rats. Second, AdipoRon restoration of cardiac Cx43 mitigates ovarian hormone-dependent LV inflammation, hypertrophy, and dysfunction. Third, while not sufficient to cause cardiac dysfunction, ovarian hormones-independent adverse effects were also alleviated by AdipoRon in T2DM OVX rats. These findings suggest that additive ovarian hormone dependent and independent molecular events contribute to the hypersensitivity of SO rats to T2DM-evoked cardiac anomalies. Further, the findings identified restoration of cardiac Cx43 as a potential therapeutic option for mitigating cardiac anomalies, particularly in E<sub>2</sub>-replete diabetic women.

Our recent study showed the first association between a reduction in cardiac Cx43 expression and the ovarian hormones (E<sub>2</sub>)-dependent hypersensitivity to T2DM-evoked cardiac hypertrophy and dysfunction (2). However, it remained unknown if Cx43 reduction contributed to these T2DM-evoked cardiac anomalies via exaggerated proinflammatory response (e.g. TNF $\alpha$ ). Consistent with our previous findings (2), we show a hypersensitivity to T2DM-evoked LV hypertrophy (Figure 2B) and LV dysfunction, which included reduced fractional shortening (Figure 2D), LVDP (Figure 3A), dP/dt<sub>max</sub> (Figure 3C) and dP/dt<sub>min</sub> (Figures 3D) in T2DM SO.

Evidence suggests that reductions in cardiac Cx43 create a proinflammatory environment, at least partly, via increased TNF $\alpha$  (27), a potent pro-inflammatory cytokine involved in T2DM associated pathogenesis (28). Here, we show the first evidence of inverse relationship between reduced Cx43 (Figure 4C) and increased TNF $\alpha$  (Figure 6A) in T2DM SO, but not in T2DM OVX, rats. These novel findings suggest that the lower cardiac TNF $\alpha$  in SO than in OVX rats paradoxically predisposes to the appreciable T2DM-evoked increase in cardiac TNF $\alpha$  and likely explains the ovarian hormones/E<sub>2</sub>-dependent hypersensitivity to T2DM evoked cardiac dysfunction. It is also imperative to note that the higher TNF $\alpha$  and asymmetric dimethylarginine (ADMA) in OVX rats might have dampened the induction of these proinflammatory molecules (Figures 5D and 6A, C) and limited the magnitude of cardiac dysfunction to a reduction in dP/dt<sub>max</sub> in T2DM OVX rats (Figures 2 and 3). These findings add new dimensions to the role of sex-dependent alterations in cardiac TNF $\alpha$  signaling in diabetic rodents (29) and likely contribute to the higher cardiac levels of other redox enzymes such as the inducible heme oxygenase 1 (HO-1) in OVX rats (Figure 6B).

While the role of HO-1 remains controversial, its elevation in diabetes (30) supports a proinflammatory role and likely explains two new findings. First, consistent with a higher vascular HO-1 (31), we show higher cardiac HO-1 (Figure 6B) in non-diabetic OVX rats. These findings suggest a mitigating effect for ovarian hormones/E<sub>2</sub> on HO-1 expression and its proinflammatory contribution to the higher vascular (31) ROS in OVX rats. Second, the ovarian hormones-independent elevation in cardiac HO-1 (Figure 6B) likely resulted from the similar hyperglycemia in T2DM SO and T2DM OVX rats (2). In support of this premise, hyperglycemia induces HO-1 in cultured cells (32, 33). Collectively, the elevation in HO-1, which reduces cardiac contractility (34), likely exaggerates cardiac dysfunction caused by other molecular responses in T2DM SO rats and contributes to the ovarian hormones-independent reduction in dP/dt<sub>max</sub> in T2DM OVX rats (Figure 3C). The latter may progress to, and likely explains, the cardiac dysfunction observed in male rats over longer T2DM timelines (35).

The findings, discussed above, identified the compromised cardiac APN-CX43 signaling as a plausible cause for the ovarian hormones-dependent hypersensitivity to T2DM-evoked cardiac inflammation and dysfunction. To ascertain this causal role, we tested the hypothesis that pharmacological restoration of the compromised APN-Cx43 signaling will mitigate this anomaly in our model system. Although APN ameliorates cardiac remodeling in pathological states (36, 37), the therapeutic benefit of exogenous APN is limited due to its short half-life, high molecular weight and its parenteral use (7, 18). Therefore, we utilized, for the first time in our model system, the orally active small molecule APN mimetic, AdipoRon, which represents a more clinically feasible alternative to APN (15).

AdipoRon mitigated the LV hypertrophy (Figure 2B) and LV anomalies in T2DM SO females including reversal of the reductions in fractional shortening (Figure 2D), LVDP (Figure 3A),  $dP/dt_{max}$  (Figure 3C),  $dP/dt_{min}$  (Figure 3D) and the prolongation of the LV relaxation constant, Tau (Figure 3B), which reflects LV chamber stiffness (25). Most notable, at the molecular level, were the restoration of Cx43 (Figure 4C and E) and the reversal of elevations of serum ADMA (Figure 5D) and cardiac TNF $\alpha$  (Figure 6A) and HO-1 (Figure 6B) in the same T2DM SO rats. It was comforting to observe these favorable molecular and functional outcomes after only 10 days of AdipoRon therapy in a model of established T2DM-evoked cardiac inflammation and dysfunction. It is likely that the pre-existing substantially suppressed APN-CX43 signaling and the associated heightened proinflammatory milieu contributed to the rapidly developing therapeutic effects of AdipoRon in T2DM SO rats. While these findings affirmed our hypothesis, it was important to study the effects of AdipoRon in T2DM OVX rats to discern its therapeutic benefit, if any, in T2DM under ovarian hormones deficient conditions and to facilitate data interpretation.

T2DM-evoked cardiac dysfunction is a slowly progressing condition because it is virtually absent at 4 weeks in OVX (Figures 2D and 3A, B and D) and in male (2) rats, but becomes evident at 8-10 weeks in male rats (35). Here, we show ovarian hormones-independent increases in proinflammatory mediators such as circulating ADMA (Figure 5D) and HO-1 expression (Figure 6B). These responses likely predispose to cardiac dysfunction in OVX, and perhaps in male (35), rats with increased exposure to T2DM. Interestingly, AdipoRon mitigated these molecular responses, as well as the reduced  $dP/dt_{max}$ , which was not sufficient to cause frank cardiac dysfunction in T2DM OVX rats. These findings infer that anti-inflammatory effects of AdipoRon (15) will likely slow or abrogate the progression of T2DM-evoked cardiac dysfunction in ovarian hormones deficient, and male, T2DM rats. While our the parallel reductions in cardiac Cx43 and phosphorylated Akt in SO T2DM rats (Figures 4C, D) agree with a similar link between both molecules under ischemia/reperfusion conditions (20), Cx43 restoration by AdipoRon was not associated with pAkt restoration. It is notable that ovarian hormones influence the roles of Cx43 (2) and pAkt (21) under different experimental conditions. More studies on these molecular responses are needed to further current understanding of the role of ovarian hormones, particularly E<sub>2</sub>, in this clinically relevant problem. Nonetheless, we considered the possibilities that alterations in ER subtypes, which modulate cardiac APN-Cx43 signaling, redox enzymes and function might be targeted by AdipoRon in ovarian hormones-dependent manner in diabetic females.



$E_2$  activation of  $ER\alpha$  confers cardioprotection via enhanced redox enzymes (catalase and ALDH<sub>2</sub>) catalytic activity (5). Paradoxically, the activation of upregulated cardiac  $ER\alpha$  by endogenous or exogenous  $E_2$  in the present and recent studies (2) likely contributed to the ovarian hormones-dependent cardiac dysfunction in T2DM female rats (Figures 2D and 3A-D). In support of this premise, similar cardiac  $ER\alpha$  upregulation (Figure 4A) occurred in T2DM females regardless of the hormonal status (2), but functional deficits manifest only in the presence  $E_2$  (Figures 2D and 3A-D) (2, 26, 38). Similar to  $ER\alpha$ , GPER physiologically confers cardioprotection (39, 40), but its role is less understood under proinflammatory conditions. Our pharmacological findings suggest a detrimental role for  $ER\alpha$ , while suggesting a favorable role for GPER, upregulation because AdipoRon: (i) reversed the upregulation of  $ER\alpha$ , and (ii) augmented GPER upregulations (Figure 4B) along with restoring cardiac function (Figures 2D and 3A-D) in diabetic rats. These molecular responses likely resulted, at least partly, from interaction between AdipoR1 (activated by AdipoRon) and  $ER\alpha$  and GPER whose endogenous ligand  $E_2$  enhances APN release (8, 41). Further, the reductions in cardiac APN and its receptor AdipoR1 levels by AdipoRon, an APN mimetic (Figure 5A and B) are consistent with pharmacological principles.

The current findings provided new insight into the role of TNF $\alpha$  and other proinflammatory signaling as major players in the ovarian hormones-dependent hypersensitivity to T2DM-evoked cardiac dysfunction. We also showed the involvement of ovarian hormones-independent increases in cardiac HO-1 expression as an additive proinflammatory component and perhaps as a predisposing factor for the delayed expression of cardiac dysfunction in T2DM OVX rats. The ability of AdipoRon to ameliorate proinflammatory cardiac milieu and dysfunction supports our scientific premise and an overall suggested schematic is presented in Figure 7. Further, the findings highlight cardiac APN-Cx43 signaling as a novel target for developing therapeutics for the treatment of the exacerbated cardiomyopathy in T2DM women.

## Acknowledgements

The authors thank Ms. Kui Sun for her technical assistance.

Partly supported by National Institutes of Health grant [2R01 AA14441-12].

## Nonstandard Abbreviations:

<b>AdipoR1</b>	adiponectin receptor 1
<b>ADMA</b>	asymmetric dimethylarginine
<b>Akt</b>	protein kinase B
<b>APN</b>	adiponectin
<b>Cx43</b>	connexin43
<b>DM</b>	diabetes mellitus/diabetic, used interchangeably with T2DM
<b><math>E_2</math></b>	estrogen/estradiol

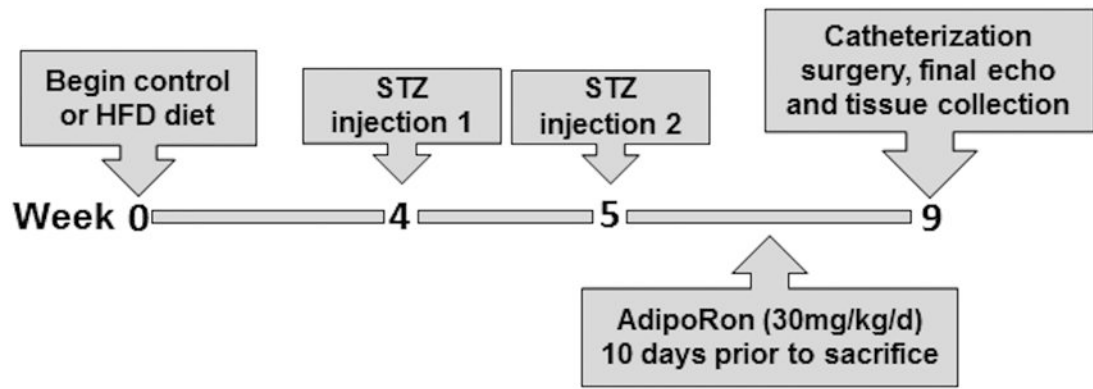
<b>ER<math>\alpha</math></b>	estrogen receptor alpha
<b>ER<math>\beta</math></b>	estrogen receptor beta
<b>ERK</b>	extracellular regulating kinases
<b>ERT</b>	estrogen replacement therapy
<b>GPER</b>	g-protein coupled estrogen receptor/GPR30
<b>HO-1</b>	heme oxygenase 1
<b>LV</b>	left ventricular
<b>LVDP</b>	left ventricular developed pressure
<b>OVX</b>	ovariectomy
<b>SO</b>	sham operated
<b>STZ</b>	streptozotocin
<b>T2DM</b>	type 2 diabetes mellitus
<b>TNF<math>\alpha</math></b>	tumor necrosis factor alpha

## References

1. Regensteiner JG, Golden S, Huebschmann AG, Barrett-Connor E, Chang AY, Chyun D, Fox CS, Kim C, Mehta N, Reckelhoff JF, Reusch JEB, Rexrode KM, Sumner AE, Welty FK, Wenger NK, Anton B, American Heart Association Diabetes Committee of the Council on Lifestyle and Cardiometabolic Health CoEaP, Council on Functional Genomics and Translational Biology, and Council on Hypertension. Sex Differences in the Cardiovascular Consequences of Diabetes Mellitus: A Scientific Statement From the American Heart Association. *Circulation*. 2015;132(25):2424–47. [PubMed: 26644329]
2. Leffler KE, Abdel-Rahman AA. Estrogen-Dependent Disruption of Adiponectin-Connexin43 Signaling Underlies Exacerbated Myocardial Dysfunction in Diabetic Female Rats. *The Journal of pharmacology and experimental therapeutics*. 2019;368(2):208–17. [PubMed: 30523063]
3. Juutilainen A, Kortelainen S, Lehto S, Ronnema T. Gender Difference in the Impact of Type 2 Diabetes on Coronary Heart Disease Risk. *Diabetes Care*. 2004;27(12):2898–904. [PubMed: 15562204]
4. Lee T-M, Lin S-Z, Chang N-C. Both GPER and membrane oestrogen receptor- $\alpha$  activation protect ventricular remodelling in 17 $\beta$  oestradiol-treated ovariectomized infarcted rats. *Journal of Cellular and Molecular Medicine*. 2014;18(12):2454–65. [PubMed: 25256868]
5. Steagall RJ, Yao F, Shaikh SR, Abdel-Rahman AA. Estrogen receptor  $\alpha$  activation enhances its cell surface localization and improves myocardial redox status in ovariectomized rats. *Life Sciences*. 2017;182:41–49. [PubMed: 28599865]
6. Tomicek NJ, Hunter JC, Machikas AM, Lopez V, Korzick DH. Acute adiponectin delivery is cardioprotective in the aged female rat heart: Adiponectin, cardioprotection and aging. *Geriatrics & Gerontology International*. 2015;15(5):636–46. [PubMed: 25115935]
7. Kadowaki T, Yamauchi T, Kubota N, Hara K, Ueki K, Tobe K. Adiponectin and adiponectin receptors in insulin resistance, diabetes, and the metabolic syndrome. *The Journal of clinical investigation*. 2006;116(7):1784–92. [PubMed: 16823476]

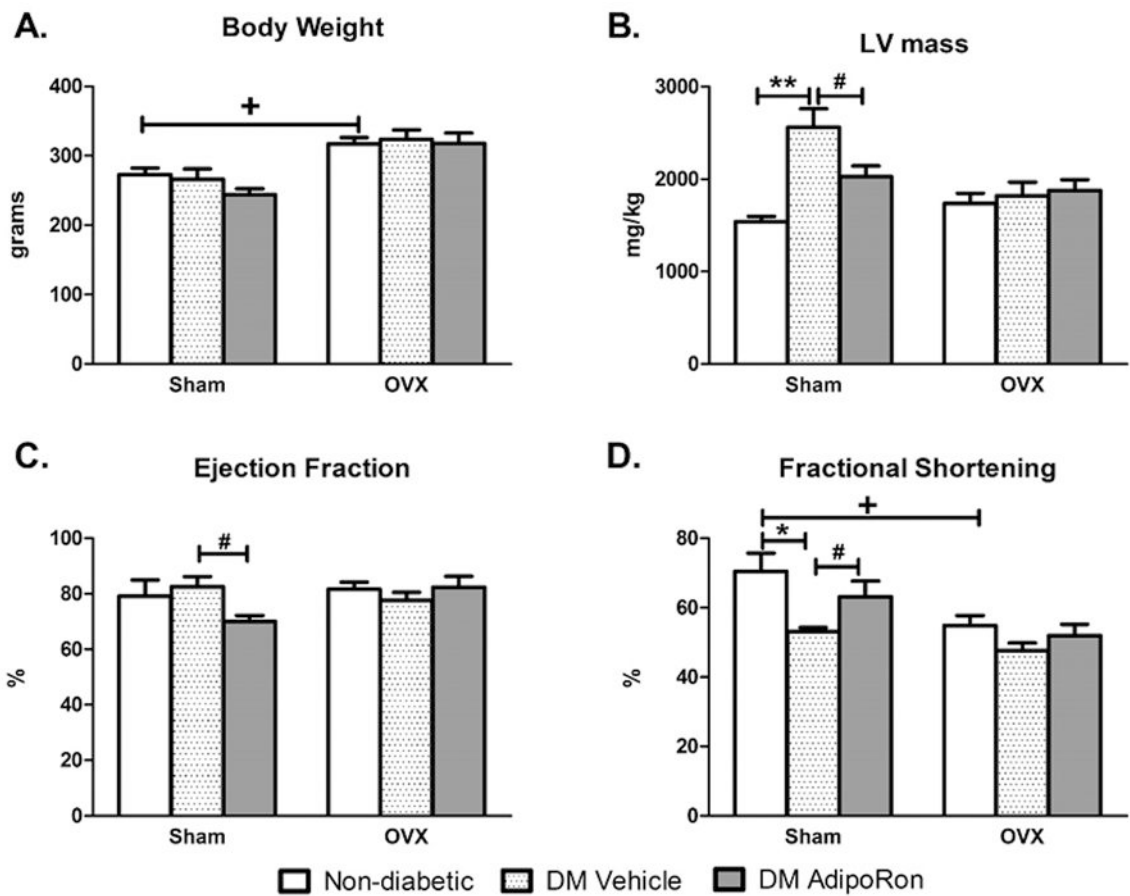
8. Zhu W, Cheng KKY, Vanhoutte PM, Lam KSL, Xu A. Vascular effects of adiponectin: Molecular mechanisms and potential therapeutic intervention. *Clinical Science*. 2008;114(5-6):361–74. [PubMed: 18230060]
9. Guo Z, Xia Z, Yuen VG, McNeill JH. Cardiac expression of adiponectin and its receptors in streptozotocin-induced diabetic rats. *Metabolism*. 2007;56(10):1363–71. [PubMed: 17884446]
10. Scherthaner G-H, Stangl H. Reduced adiponectin receptor signalling accelerates atherosclerosis and may worsen the outcome in type 2 diabetes mellitus – Another one of those missing links? *Atherosclerosis*. 2013;229(1):30–31. [PubMed: 23545182]
11. Ruiz-Meana M, Rodriguez-Sinovas A, Cabestrero A, Boengler K, Heusch G, Garcia-Dorado D. Mitochondrial connexin43 as a new player in the pathophysiology of myocardial ischaemia-reperfusion injury. *Cardiovascular Research*. 2008;77(2):325–33. [PubMed: 18006437]
12. Bikou O, Thomas D, Trappe K, Lugenbiel P, Kelemen K, Koch M, Soucek R, Voss F, Becker R, Katus HA, Bauer A. Connexin 43 gene therapy prevents persistent atrial fibrillation in a porcine model. *Cardiovascular Research*. 2011;92(2):218–25. [PubMed: 21799069]
13. Stauffer BL, Sobus RD, Sucharov CC. Sex Differences in Cardiomyocyte Connexin43 Expression. *Journal of Cardiovascular Pharmacology*. 2011;58(1):32–9. [PubMed: 21753256]
14. Gourdie RG. The Cardiac Gap Junction has Discrete Functions in Electrotonic and Ephaptic Coupling. *The Anatomical Record*. 2019;302(1):93–100. [PubMed: 30565418]
15. Okada-Iwabu M, Yamauchi T, Iwabu M, Honma T, Hamagami K-I, Matsuda K, Yamaguchi M, Tanabe H, Kimura-Someya T, Shirouzu M, Ogata H, Tokuyama K, Ueki K, Nagano T, Tanaka A, Yokoyama S, Kadowaki T. A small-molecule AdipoR agonist for type 2 diabetes and short life in obesity. *Nature*. 2013;503(7477):493–9. [PubMed: 24172895]
16. Zhang Y, Zhao J, Li R, Lau WB, Yuan Y-X, Liang B, Li R, Gao E-H, Koch WJ, Ma X-L, Wang Y-J. AdipoRon, the first orally active adiponectin receptor activator, attenuates posts ischemic myocardial apoptosis through both AMPK-mediated and AMPK-independent signalings. *American Journal of Physiology - Endocrinology and Metabolism*. 2015;309(3):E275–E82. [PubMed: 26037251]
17. Lin L-C, Wu C-C, Yeh H-I, Lu L-S, Liu Y-B, Lin S-F, Lee Y-T. Downregulated myocardial connexin 43 and suppressed contractility in rabbits subjected to a cholesterol-enriched diet. *Laboratory Investigation*. 2005; 85: 1224–1237. [PubMed: 16127430]
18. Zhang N, Wei W-Y, Liao H-H, Yang Z, Hu C, Wang S-s, Deng W, Tang Q-Z. AdipoRon, an adiponectin receptor agonist, attenuates cardiac remodeling induced by pressure overload. *Journal of Molecular Medicine*. 2018;96(12):1345–57. [PubMed: 30341569]
19. Choi BS, Choi SR, Lim K-M, Lim JH, Kim Y-S, Kim MJ, Kim EN, Kim Y, Kim HW, Kim MY, Park CW. Adiponectin receptor agonist AdipoRon decreased ceramide, and lipotoxicity, and ameliorated diabetic nephropathy. *Metabolism*. 2018;85:348–60. [PubMed: 29462574]
20. Solan JL, Márquez-Rosado L, Lampe PD. Cx43 phosphorylation-mediated effects on ERK and Akt protect against ischemia reperfusion injury and alter the stability of the stress-inducible protein NDRG1. *The Journal of biological chemistry*. 2019;294(31):11762–71. [PubMed: 31189653]
21. Abdel-Rahman AA. Influence of sex on cardiovascular drug responses: role of estrogen. *Current Opinion in Pharmacology*. 2017;33:1–5. [PubMed: 28340373]
22. El-Mas M, Abdel-Rahman A. Ovariectomy alters the chronic hemodynamic and sympathetic effects of ethanol in radiotelemetered female rats. *Clinical & Experimental Hypertension*. 2000 01//;22(1):109. [PubMed: 10685729]
23. Brown L, Panchal SK. Rodent models for metabolic syndrome research. *Journal of Biomedicine and Biotechnology*. 2011;1–14. [PubMed: 21836813]
24. Sasidharan SR, Joseph JA, Anandakumar S, Venkatesan V, Ariyattu Madhavan CN, Agarwal A. An Experimental Approach for Selecting Appropriate Rodent Diets for Research Studies on Metabolic Disorders. *BioMed Research International*. 2013:1–9.
25. Flachskampf FAMDP, Biering-Sørensen TMDP, Solomon SDMD, Duvernoy OMDP, Bjerner TMDP, Smiseth OAMDP, Medicinska f. Medicinska och farmaceutiska v, Kardiologi, Uppsala u, Institutionen för medicinska v, Institutionen för kirurgiska v, Radiologi. Cardiac Imaging to Evaluate Left Ventricular Diastolic Function. *JACC: Cardiovascular Imaging*. 2015;8(9):1071–93. [PubMed: 26381769]

26. Yao F, Abdel-Rahman AA. Estrogen Receptors  $\alpha$  and  $\beta$  Play Major Roles in Ethanol-Evoked Myocardial Oxidative Stress and Dysfunction in Conscious Ovariectomized Rats. *Alcoholism: Clinical and Experimental Research*. 2017;41(2):279–90.
27. Okruhlicova L, Cicakova Z, Frimmel K, Weismann P, Krizak J, Sotnikova R, Knezl V, Slezak J. Lipopolysaccharide-induced redistribution of myocardial connexin43 is associated with increased macrophage infiltration in both normotensive and spontaneously hypertensive rats. *Journal of physiology and pharmacology : an official journal of the Polish Physiological Society*. 2018 10;69(5).
28. Yamakawa I, Kojima H, Terashima T, Katagi M, Oi J, Urabe H, Sanada M, Kawai H, Chan L, Yasuda H, Maegawa H, Kimura H. Inactivation of TNF- $\alpha$  ameliorates diabetic neuropathy in mice. *American Journal of Physiology - Endocrinology and Metabolism*. 2011;301(5):E844–E52. [PubMed: 21810933]
29. Delgado C, Gomez A-M, Samia El Hayek M, Ruiz-Hurtado G, Pereira L. Gender-Dependent Alteration of Ca<sup>2+</sup> and TNF $\alpha$  Signaling in db/db Mice, an Obesity-Linked Type 2 Diabetic Model. *Frontiers in Physiology*. 2019;10:40. [PubMed: 30792662]
30. Maamoun H, Benameur T, Pintus G, Munusamy S, Agouni A. Crosstalk Between Oxidative Stress and Endoplasmic Reticulum (ER) Stress in Endothelial Dysfunction and Aberrant Angiogenesis Associated With Diabetes: A Focus on the Protective Roles of Heme Oxygenase (HO)-1. *Frontiers in Physiology*. 2019; 10(70):1–21. [PubMed: 30723415]
31. Lee Y-M, Cheng P-Y, Hong S-F, Chen S-Y, Lam K-K, Sheu J-R, Yen M-H. Oxidative stress induces vascular heme oxygenase-1 expression in ovariectomized rats. *Free Radical Biology and Medicine*. 2005;39(1):108–17. [PubMed: 15925283]
32. Fouda MA, Abdel-Rahman AA. Endothelin Confers Protection against High Glucose-Induced Neurotoxicity via Alleviation of Oxidative Stress. *J Pharmacol Exp Ther*. 2017 4;361(1):130–9. [PubMed: 28179472]
33. Wang H-h, Sun P-f, Chen W-k, Zhong J, Shi Q-q, Weng M-l, Ma D, Miao C-h. High Glucose Stimulates Expression of MFHAS1 to Mitigate Inflammation via Akt/HO-1 Pathway in Human Umbilical Vein Endothelial Cells. *Inflammation*. 2018;41(2):400–8. [PubMed: 29168081]
34. Achouh P, Simonet S, Badier-Commander C, Chardigny C, Vayssettes-Courchay C, Zegdi R, Khabbaz Z, Fabiani J-N, Verbeuren TJ. The induction of heme oxygenase 1 decreases contractility in human internal thoracic artery and radial artery grafts. *The Journal of Thoracic and Cardiovascular Surgery*. 2005;130(6):1573–80. [PubMed: 16308001]
35. Hoit BD, Castro C, Bultron G, Knight S, Matlib MA. Noninvasive evaluation of cardiac dysfunction by echocardiography in streptozotocin-induced diabetic rats. *Journal of Cardiac Failure*. 1999/12/01;5(4):324–33. [PubMed: 10634674]
36. Takemura Y, Ouchi N, Shibata R, Aprahamian T, Kirber MT, Summer RS, Kihara S, Walsh K. Adiponectin modulates inflammatory reactions via calreticulin receptor-dependent clearance of early apoptotic bodies. *The Journal of clinical investigation*. 2007;117(2):375–86. [PubMed: 17256056]
37. Tian L, Luo N, Klein RL, Chung BH, Garvey WT, Fu Y. Adiponectin reduces lipid accumulation in macrophage foam cells. *Atherosclerosis*. 2009;202(1):152–61. [PubMed: 18511057]
38. White RE, Han G, Dimitropoulou C, Zhu S, Miyake K, Fulton D, Dave S, Barman SA. Estrogen-induced contraction of coronary arteries is mediated by superoxide generated in vascular smooth muscle. *American Journal of Physiology - Heart and Circulatory Physiology*. 2005;289(4):H1468–H75. [PubMed: 16162867]
39. Deschamps AM, Murphy E. Activation of a novel estrogen receptor, GPER, is cardioprotective in male and female rats. *American Journal of Physiology - Heart and Circulatory Physiology*. 2009;297(5):1806–13.
40. Li W-L, Xiang WEI, Ping YE. Activation of novel estrogen receptor GPER results in inhibition of cardiocyte apoptosis and cardioprotection. *Molecular Medicine Reports*. 2015;12(2):2425–30. [PubMed: 25936661]
41. Fisman EZ, Tenenbaum A. Adiponectin: a manifold therapeutic target for metabolic syndrome, diabetes, and coronary disease? *Cardiovasc Diabetol*. 13:103:1-10. [PubMed: 24957699]



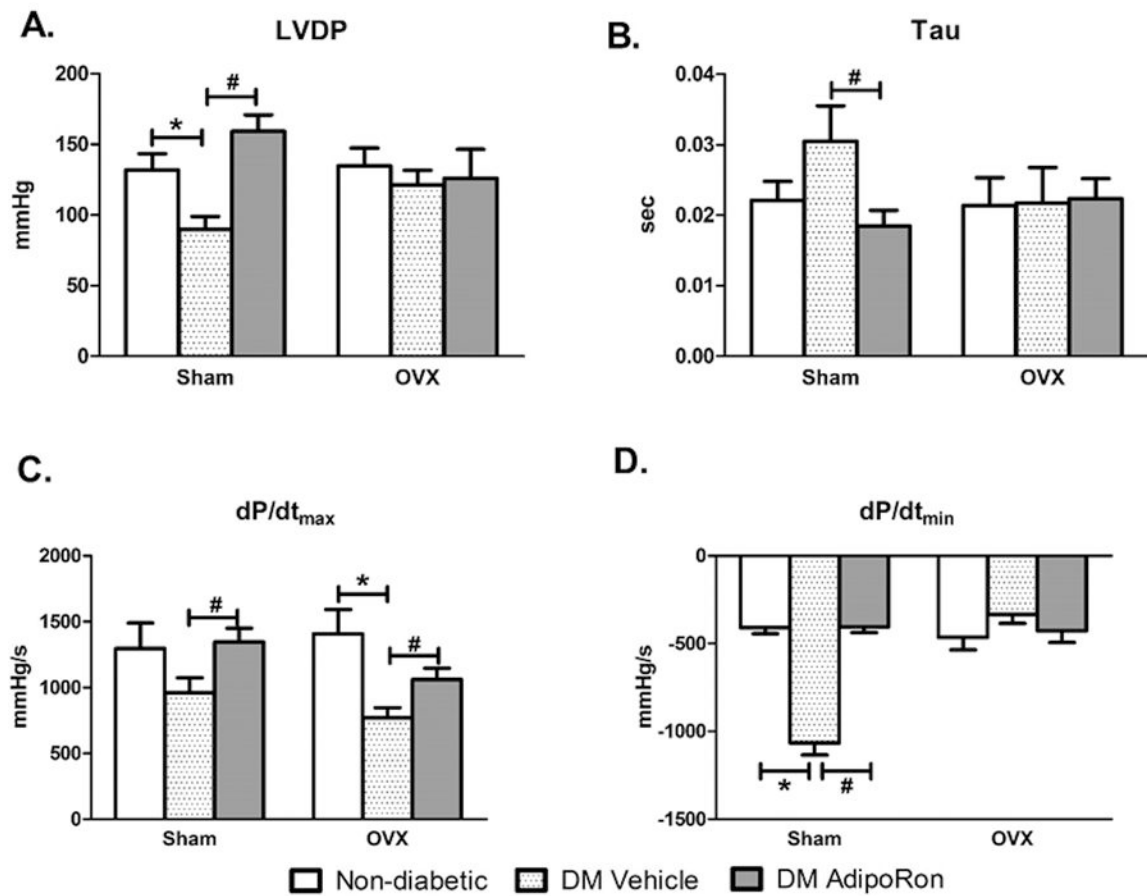
**Figure 1.**

A schematic presentation of experimental diet regimen, T2DM induction, treatment schedule and the biochemical and molecular cardiovascular measurements in control and diabetic Wistar rats. OVX, ovariectomy; STZ, streptozotocin.

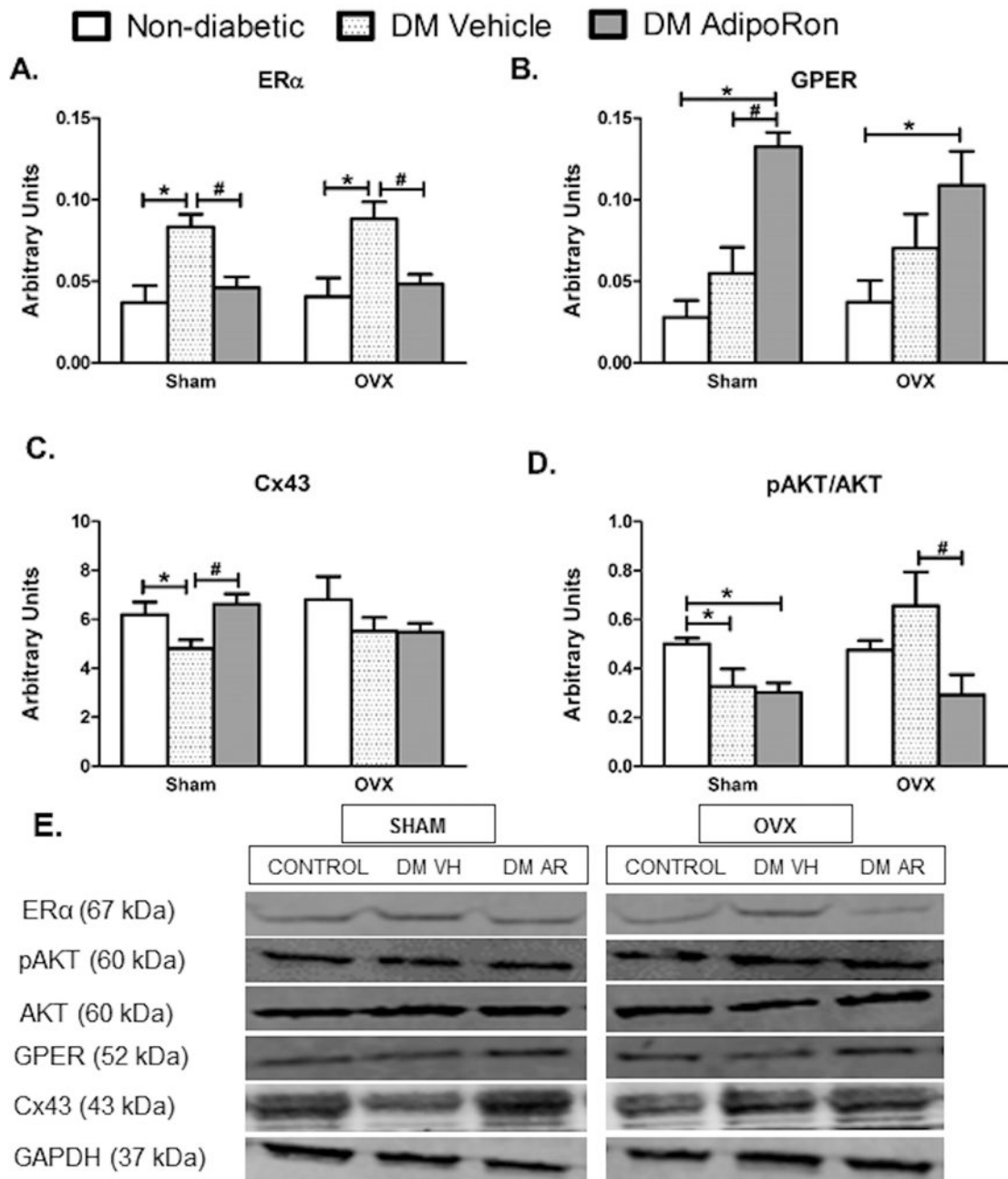
**Figure 2.**

Effect of diabetes on animal body weight (A), echocardiography-derived left ventricular mass (B), ejection fraction (C) and fractional shortening (D) in non-diabetic sham or ovariectomized (OVX) controls (open bars), and in vehicle (dotted bars) and AdipoRon (dark bars) treated diabetic rats. AdipoRon attenuated the detrimental cardiac effects of diabetes in sham rats. Values are means  $\pm$  SEM (n=7 per group). \*P<0.05 when compared to respective control, \*\*P<0.001 when compared to respective control, #P<0.05 when compared to T2DM vehicle group and +P<0.05 when compared to control sham rats.

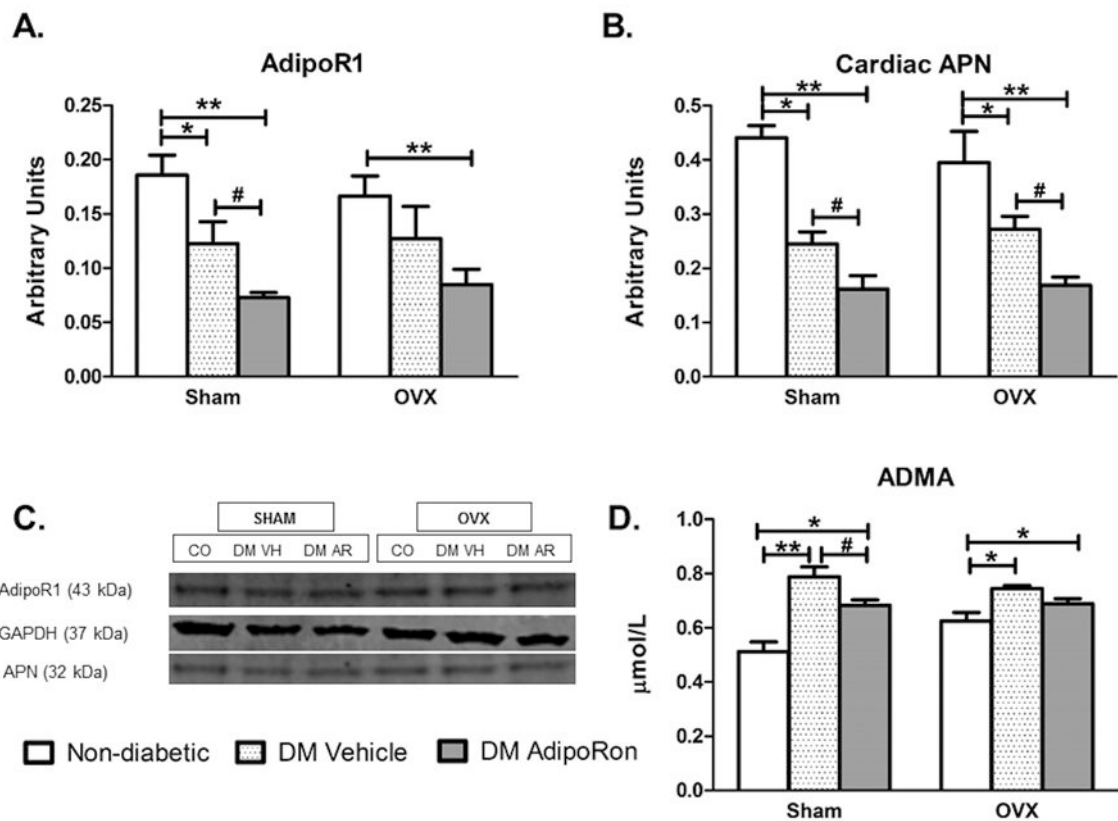


**Figure 3.**

Effect of diabetes on blood pressure-derived hemodynamic variables. Diabetic (T2DM) sham operated (SO) females display significant differences in left ventricular developed pressure (LVDP) (A), Tau (B),  $dP/dt_{max}$  (C) and  $dP/dt_{min}$  (D) with AdipoRon treatment. Values are means  $\pm$  SEM (n=7 per group). \*P<0.05 when compared to respective non-diabetic control (open bars); #P<0.05 when AdipoRon (dark bars) and vehicle (dotted bars) treated T2DM groups were compared.

**Figure 4.**

Western blots of cardiac estrogen receptors (ERs), connexin43 (Cx43) and AKT in control and diabetic (vehicle or AdipoRon treated) female rats. Shown are alterations in ER $\alpha$  (A), G-protein coupled estrogen receptor; GPER (B), Cx43 (C), and pro-survival molecule pAKT (D). Data presented as means  $\pm$  SEM (n=7 per group). Representative blots are shown (E) and target bands were normalized to GAPDH, except for pAKT (normalized to total AKT), on the same gel. \*P<0.05 when compared to respective non-diabetic control (open bars); #P<0.05 when AdipoRon (dark bars) and vehicle (dotted bars) treated T2DM groups were compared.

**Figure 5.**

Cardiac adiponectin receptor 1 (AdipoR1) (A) and adiponectin (APN) (B) and plasma ADMA (C) levels in diabetic (T2DM) sham operated (SO) and ovariectomized (OVX) rats, compared with their respective controls and following treatment with AdipoRon or its vehicle in T2DM SO and OVX rats. Representative blots are shown (D). Data presented as means  $\pm$  SEM (n=7 per group). \*P<0.05 when compared to respective control (open bars); \*\*P<0.001 when compared to respective non-diabetic control and #P<0.05 when AdipoRon (dark bars) and vehicle (dotted bars) treated T2DM groups were compared.

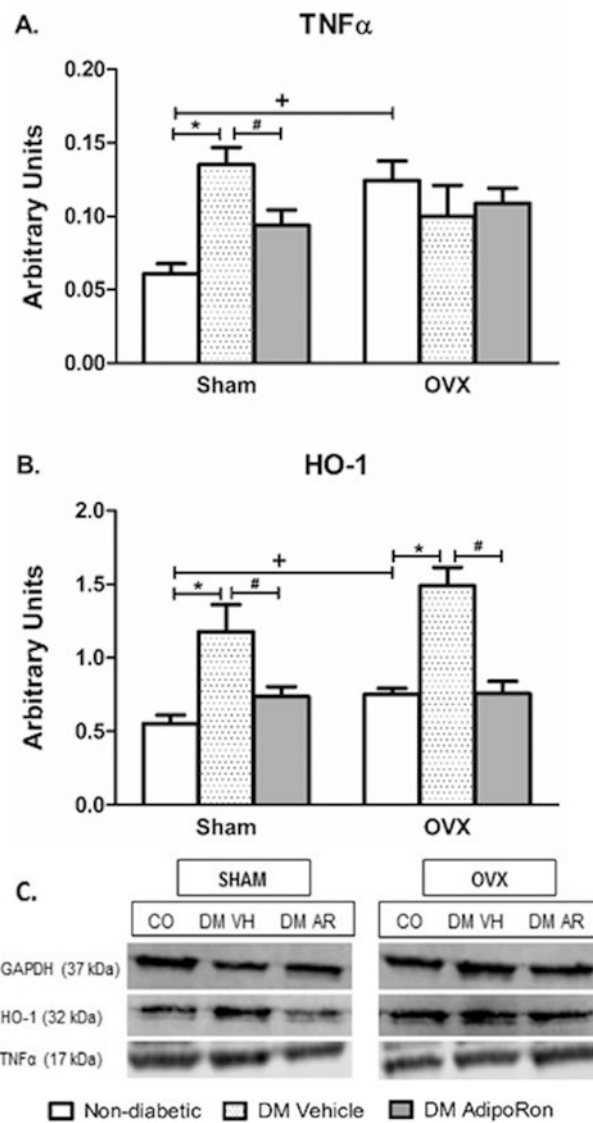


**Figure 6.** Cardiac levels of TNF $\alpha$  (A), HO-1 (B), their representative bands (C) in non-diabetic sham operated (SO) and ovariectomized (OVX), and in vehicle- or AdipoRon-treated diabetic (T2DM) SO and OVX rats. Data presented as means  $\pm$  SEM (n=7 per group). \*P<0.05 when compared to respective control (open bars); \*\*P<0.001 when compared to respective non-diabetic control and #P<0.05 when AdipoRon (dark bars) and vehicle (dotted bars) treated T2DM groups were compared, and +P<0.05 when compared to control sham operated (SO).

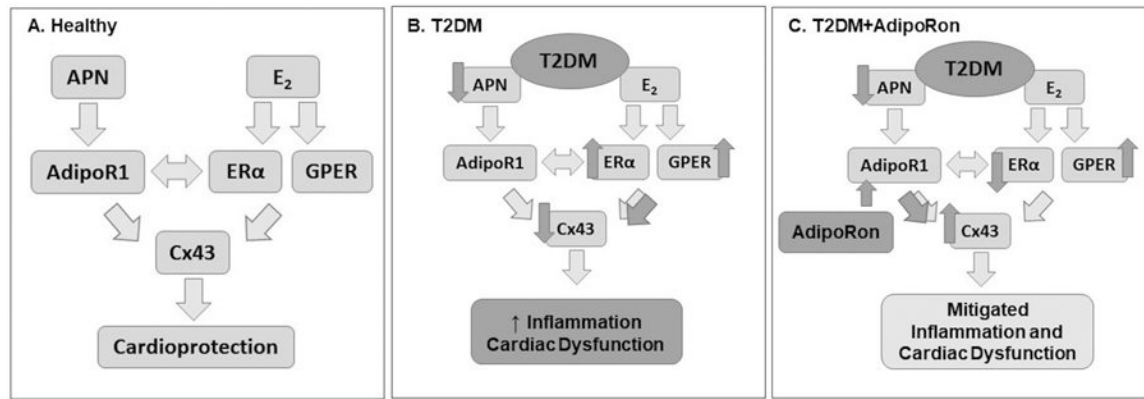


**Figure 7.**

Suggested Overall Schematic. Healthy female signaling in the cardiac E<sub>2</sub>-APN-Cx43 axis (A). The loss of this cardioprotection with the introduction of a diabetic pathology, leading to exacerbated myocardial anomalies (B) and the amelioration of exacerbated dysfunction with the restoration of APN-Cx43 signaling by AdipoRon in the T2DM female (C).